Towards materials with enhanced electro-mechanical response: CaCu₃Ti₄O₁₂/Polydimethylsiloxane composites

Laura J. Romasanta[a]*, Pilar Leret[b], Leandro Casaban[c], Marianella Hernández[a], Miguel A. de la Rubia[b], José F. Fernández[b], José M. Kenny[a, c], Miguel A. Lopez-Manchado[a], Raquel Verdejo[a]*

We describe a straightforward production pathway of polymer matrix composites with increased dielectric constant for dielectric elastomer actuators (DEAs). Up to date, the approach of using composites made of high dielectric constant ceramics and insulating polymers has not evidenced any improvement in the performance of DEA devices, mainly as a consequence of the ferroelectric nature of the employed ceramics. We propose here an unexplored alternative to these traditional fillers, introducing Calcium Copper Titanate (CCTO) CaCu₃Ti₄O₁₂, which has a giant dielectric constant making it very suitable for capacitive applications. All CCTO/Polydimethylsiloxane (PDMS) composites developed display an improved electro-mechanical performance. The largest actuation improvement was achieved for the composite with 5.1 vol.% of CCTO, having an increment in the actuation strain of about 100% together with a reduction of 25% in the electric field compared to the raw PDMS matrix.

1 Introduction

Soft dielectric elastomer actuators (DEAs) are a fast growing and promising scientific field of research and development due to their outstanding potential to active deformation.[1] Given their excellent properties, this class of materials enable a wide range of interesting applications, such as arm-wrestling robots,[2] fish-like propellers in airships,[3] refreshable tactile displays[4] or micro-actuators for mecano-transduction of individual cells,[5] to name but a few.

DEAs consist of a thin elastomeric film sandwiched between two compliant electrodes, thus forming a capacitor.[6] The application of an external voltage triggers the appearance of charges of opposite polarity on the electrodes, which, in turn, causes an electrical stress on the dielectric elastomeric film. This electrostatic pressure, known as Maxwell's stress, leads to a mechanical deformation of the elastomeric film, reducing its thickness while elongating it in the direction perpendicular to the electric field. The strain suffered by the elastomer is directly proportional to the electrostatic pressure and inversely proportional to the elastomer tensile stress at a given strain. Nevertheless, one of the main hindrances to the wide-spread DEA implementation is the huge voltages (several thousands of volts) required to stimulate the mechanical actuation.

We aimed to develop a straightforward and industrially scalable dielectric elastomer actuator (DEA), based on a composite approach of Polydimethylsiloxane (PDMS) with a giant dielectric permittivity filler. This paper evidences the advantages of selecting non-ferroelectric fillers for DEA devices.

2 Background

The actuator performance was derived by Pelrine *et al.*[6] from the electrostatic energy stored in an elastomer film and its mechanical response:

$$S_z = \frac{p}{Y} = \frac{\varepsilon_0 \varepsilon'}{Y}\left(\frac{V}{d}\right)^2 \qquad (1)$$

where p is the electrostatic pressure, Y the elastomer tensile stress at a given strain, ε_0 the vacuum permittivity, ε' the elastomer dielectric permittivity, V the applied voltage between the electrodes and d the thickness of the elastomeric film. This equation defines the possible approaches to reduce the large driving voltages required to actuate the elastomer film: i) reducing its thickness, ii) reducing its mechanical stiffness and iii) increasing its dielectric permittivity.

This last approach is, up to date, the most promising method and is been pursued through both the chemical grafting of polarizable organic (macro)molecules to an elastomer backbone[7] and the development of composite elastomeric systems.[8-10] The first strategy has recently shown to increase the electro-mechanical performance of certain elastomers. Nevertheless, chemical procedures involve both time-consuming and rather expensive reactions, which could hinder a timely scale-up of the developed materials. The more conventional strategy of elastomer composites presents the advantage of, on one hand, being easily scalable and, on the other, the combination of the high dielectric permittivity values of conductive and/or ceramic fillers with the high breakdown strength of polymers. Nevertheless, this strategy has also to overcome additional limitations since an ideal composite system for DEA applications should have high dielectric permittivity, low dielectric loss and low tensile stress.[11] However, composites satisfying all three characteristics are difficult to attain as the addition of these fillers is prone to increase both the dielectric loss and the tensile stress values, which can decrease, or even ruin, the electro-mechanical performance of the actuator.

Conductive fillers, such as metal particles (Ni[12] and Ag[13]), carbon black[14] and carbon nanotubes[15] or even conductive polymers such as Polyaniline (PANI),[16] have already shown to

effectively increase the dielectric permittivity of polymeric matrices but also increased the dielectric loss leading to the early breakdown of the composites, thus excluding these additives for DEA applications.

Extremely high dielectric constant fillers have always been associated with ferroelectric and/or relaxor ceramics such as $Pb(Mg_{1/3}Nb_{2/3})O_3$–$PbTiO_3$ (PMN-PT), $Pb(Zr,Ti)O_3$ (PZT) and $BaTiO_3$ (BT). The availability of these inorganic fillers together with their high dielectric constant values (on the order of hundreds or even thousands) make them very appealing to be used as high dielectric constant fillers for DEA applications. In fact, Szabo et al.,[17] Gallone et al.,[18] and more recently, Molberg et al.,[19] have reported the enhancing effect of BT, PMN-PT and PZT ceramics, respectively, on the dielectric response of different elastomers. Nevertheless, in spite of the permittivity increment observed in all the cases, these authors did not establish real improvements in the electro-mechanical performances of the developed composites mainly due to: i) the increase in the dielectric permittivity was counterbalanced by an increase in the elastic modulus, ii) the electrical breakdown strength was reduced considerably, which clearly limited the maximum performance and, finally, iii) the dielectric loss dramatically increased with the filler content cancelling the electro-mechanical performance of the actuator. Besides, the presence of a permanent dipole moment in ferroelectric metal oxides, even after removing the electric field, is able to induce a strong mechanical resonance, thus decreasing the reliability of DEA devices.[20]

An unexplored alternative to these ferroelectric ceramic particles is the use a giant permittivity ceramic system. Calcium Copper Titanate $CaCu_3Ti_4O_{12}$ (CCTO) is attracting increasing attention since Subramanian et al.[21] measured a frequency independent giant dielectric constant of 10^4 (DC to 10^6 Hz) at room temperature. CCTO ceramics possess a cubic distorted perovskite-like structure (Figure 1a) with Im3 space group.[22] The different sizes of the Ca and Cu cations and the order of the Cu^{2+} ions in a square-planar environment cause the tilting of the TiO_6 octahedra, which is large enough to accommodate local distortions, thus, ruling out the pure ferroelectric behavior in CCTO ceramics.[21] Nowadays, it is widely accepted that the high permittivity value of sintered CCTO ceramic is associated with an internal barrier layer capacitance (IBLC) structure.[23-25] In this model, the conductivity of a sample is prevented to percolate by the presence of insulating blocking layers at the surfaces or at internal domain boundaries. Thus, the behavior of CCTO can be explained in terms of semi-conducting grains surrounded by insulating grain boundaries, which makes it to be considered as a very promising high dielectric constant filler for applications in microelectronic, mainly in capacitive applications. Although the grounded CCTO powder would not present the same giant dielectric permittivity constant, the polarisability of the Ti-O bond should still be retained, making it an ideal candidate for actuators based on dielectric elastomers.

Here, the developed composites were investigated with respect to their applicability for DEAs in terms of dielectric and mechanical properties as well as their electro-mechanical behavior. Several models were applied to get a deeper understanding of both the enhancement mechanism of the dielectric permittivity in the developed composites and the corresponding change in the actuation performances. The results indicate that this strategy leads to useful materials with superior electro-mechanical response and represents a large step forward in the understanding of the suitable methods to obtain high permittivity elastomeric composites with practical uses for flexible actuators.

3 Experimental Section

3.1 Synthesis of CCTO and CCTO/PDMS composites

The stoichiometric $CaCu_3Ti_4O_{12}$ polycrystalline sample employed in this study was synthesized by a conventional solid-state reaction and sintering process.[26, 27] $CaCO_3$ (Aldrich), TiO_2 (Merck), and CuO (Aldrich) powders were mixed for 4 h by attrition milling with 1.2 mm zirconia balls, using deionized water as liquid medium and 0.2 wt.% of Dolapix C64 (Zschimmer & Schwarz) as a dispersant. The milled powders were dried and sieved through a 100 μm mesh, calcined at 900 °C for 12 h and attrition milled for 3 h. Organic binder (0.6 wt.% of polyvinyl alcohol) was added into the calcined powder upon milling to help the formation of compacts and sieved through a 63 μm mesh after drying. Dense pellets were prepared with CCTO powder by sintering uniaxially pressed compacts in air at 1000 °C during 32 h. The sintered ceramic pellets were then ground using several ball milling processes until the particle diameter corresponding to the 90% (d_{90}) of the cumulative size distributions was about 5 μm. Final CCTO powder density was measured as $\rho = 5.12$ g/cm^3 by He picnometry.

A commercial Polydimethylsiloxane kindly supplied by BlueStar Silicones (Rhodorsil MF620U) was used as elastomeric matrix. The vulcanization of this silicone was achieved by means of a bi-functional organic peroxide (0.6% of 2,5-Bis-(tert-butylperoxy)-2,5-dimethylhexane) via free-radical polymerization mechanism. Composites of 2.3, 5.1, and 8.4 vol.% of CCTO/PDMS (which correspond to 10, 20 and 30 wt.%) were prepared at room temperature in an open two-roll laboratory mill (speed ratio of 1:1.4) using standard mixing procedures. The vulcanization kinetics of PDMS and its composites were followed at 170 °C by means of a rubber process analyzer (RPA2000 Alpha Technologies) at a deformation of 6.98%, with an oscillation rate of 1.667 Hz. After that, samples were vulcanized at the same temperature and 200 bar in an electrically heated hydraulic press using the optimum cure time (t_{90}) deduced from the curing curves previously determined.

3.2 Characterization techniques

Cryo-fractured cross-sections of the vulcanized composites were examined by scanning electron microscopy (SEM), (ESEM XL30 Model, Philips). Samples were sputter-coated with a thin layer of 3-4 nm of gold/palladium lead prior to imaging.

Raman spectra were obtained using a confocal Raman microscope (Witec alpha-300R) with 532 nm excitation laser

and a 100× objective lens (NA = 0.9). The incident laser power was 0.5 mW. The optical diffraction resolution of the confocal microscope was limited to about ~200 nm laterally and ~500 nm vertically. Raman spectral resolution of the system was down to 0.02 cm^{-1}. The microscopy sample was mounted in a piezo-driven scan platform having 4 nm lateral and 0.5 nm vertical positioning accuracy. The microscope base was also equipped with an active vibration isolation system, active in the frequency range of 0.7 – 1000 Hz. Samples were mounted on a microscopy glass slide. Collected spectra were analyzed by using Witec Control Plus software.

Broadband dielectric spectroscopy was performed on an ALPHA high-resolution dielectric analyzer (Novocontrol Technologies GmbH). Vulcanized film disc-shaped samples were held in the dielectric cell between two parallel gold-plated electrodes. The thickness of the films (around 100 μm) was taken as the distance between the electrodes and determined using a micrometer gauge. The dielectric response of each sample was assessed by measuring the complex permittivity $\varepsilon^*(\omega) = \varepsilon'(\omega) - j\varepsilon''(\omega)$ over a frequency range window of 10^{-1} - 10^6 Hz at 23 °C. The amplitude of the ac electric signal applied to the samples was 1 V. In this work, the real part of the complex permittivity constant is referred simply as the dielectric permittivity. As already mentioned in the background, composites for DEA applications should be characterized by low dielectric loss. The results herein presented correspond to the loss tangent ($tan(\delta) = \varepsilon''/\varepsilon'$), since this parameter reflects simultaneously the contribution of both the dielectric permittivity and the dielectric loss.

Stress-strain measurements were performed on a tensile test machine (Instron 3366 dynamometer) at 23 °C. Dog bone shaped specimens with thickness around 0.5 mm were mechanically cut out from the vulcanized samples. The tests were carried out at a cross-head speed of 200 mm·min^{-1} with a distance between clamps of 2.0 mm. The elongation during each test was determined by optical measurement (video extensometer) of the displacement of two marker points placed along the waist of the tensile test sample. An average of five measurements for each sample was recorded.

Electro-mechanical properties were studied using planar actuator configuration. Vulcanized rectangular thin films were bi-axially pre-strained (50%) and thereafter fixed to a supporting hard plastic frame. This pre-strain should prevent any issues related to pull-in effects.[28] Compliant circular electrodes (6 mm diameter) were sprayed on each side of the film using a suspension of graphite powder (purum powder ≤ 0.1 mm, Fluka) in ethanol and leaving 2 cm free area near the edges to prevent arcing. Thin aluminum stripes were then glued with silver paint to the circular electrodes, in order to ensure electrical connection with the high voltage supply (SL30PN600 model, Spellman Corp.). Actuator performance tests were carried out applying an increasing ramp voltage until breakdown. The actuation strain was optically measured with a digital microscope using a modified edge detection tool of LabView. Actuated relative area strain percentages as a function of the nominal electric field applied were calculated using the variation of the radius value of the electrode area.[6]

4 Results and Discussion

4.1 Synthesis of CaCu₃Ti₄O₁₂ (CCTO)

The polycrystalline $CaCu_3Ti_4O_{12}$ employed in this work was prepared by a traditional solid-state reaction followed by a sintering process.[26, 27] The formation of the CCTO ceramic was confirmed via powder X-ray diffraction (see ESI for the X-ray patterns). The microstructure of the sintered ceramic pellets was composed of n-type semi-conducting grains with an average particle size of 15 μm, surrounded of insulating grain boundaries with a thickness ≤ 10 nm. In order to incorporate the CCTO in the elastomeric matrix, the sintered ceramic pellets were subjected to several grounding processes to reduce the particle size. This process reduced the CCTO grain size, until the particle diameter corresponding to the 90% (d_{90}) of the cumulative size distributions was about 5 μm (Figure 1b). Figure 1c and 1d show the dependence of the dielectric permittivity (ε') and the loss tangent ($tan(\delta)$) with the frequency for both the sintered CCTO pellet and the final CCTO powder obtained. As can be seen in Figure 1c, CCTO pellet possess a giant dielectric permittivity in good agreement with previous works that validate the quality of the starting CCTO ceramics.[21, 29, 30] As expected, CCTO powder shows lower dielectric permittivity values compared to the sintered sample as a result of the microstructure deconstruction. The lower dielectric permittivity value of CCTO powder is caused by the lower density of the material in this aggregation state. Ceramic CCTO (pellet) is a dense material with a density value over 95% of the theoretical one, while CCTO ceramic powder, even if it very well pressed and compacted, is not a dense material.
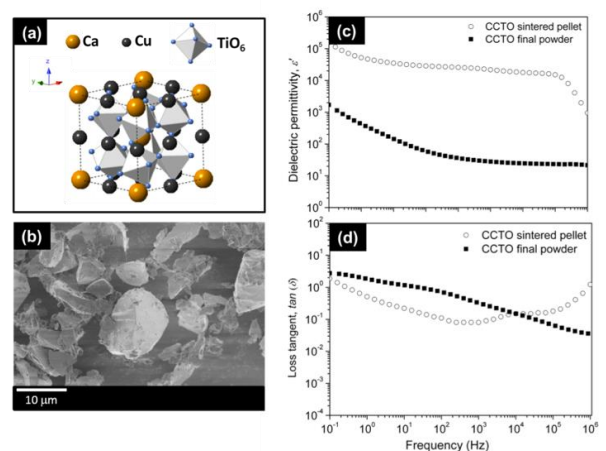
Fig. 1 (a) Unit cell structure of $CaCu_3Ti_4O_{12}$ (CCTO). (b) SEM micrograph of CCTO powder (the scale bar corresponds to 10 μm). (c) Dielectric permittivity and (d) loss tangent values for CCTO after the sintering and the grounding processes.

Table 1 Vulcanization kinetic parameters (S'_{max}, t_{90}), tensile stress values (σ) at different strain levels (50, 100 and 300%) and elongation at break (e_b) values.

Sample	S'_{max} (dNm)	t_{90} (min)	$\sigma_{50\%}$ (MPa)	$\sigma_{100\%}$ (MPa)	$\sigma_{300\%}$ (MPa)	e_b (%)
PDMS	3.96	2.47	0.29 ± 0.01	0.37 ± 0.02	0.86 ± 0.04	711 ± 30
2.3 vol.% CCTO	3.78	2.28	0.29 ± 0.02	0.38 ± 0.02	0.87 ± 0.04	699 ± 43
5.1 vol.% CCTO	4.32	2.13	0.29 ± 0.01	0.38 ± 0.01	0.83 ± 0.03	745 ± 49
8.4 vol.% CCTO	4.64	2.02	0.36 ± 0.03	0.48 ± 0.03	1.02 ± 0.07	740 ± 36

Nevertheless, the tension in the Ti-O bonds and, hence, the remarkable polarizability of the CCTO should still be preserved in the powder sample. The powder fracture surfaces of the semi-conducting grains should be able to form polymer/filler interfaces that in fact became insulating/semi-conductor interfaces. We propose that these new interfaces could play a significant role in the electro-mechanical performances of the actuators here developed.

4.2. CCTO/Polydimethylsiloxane Composites

### 4.2.1. Vulcanization Process and Mechanical Properties

After incorporating the CCTO ceramic micro-particles in the elastomeric matrix, the vulcanization kinetics of the materials were measured by an oscillating disk curemeter at 170 ºC. The vulcanization process is characterized by the maximum torque (S'_{max}) achieved during the process and the optimum cure time, t_{90}, which is the time necessary to achieve 90 % of the maximum torque. The results in Table 1 show that the incorporation of CCTO micro-particles slightly increases the maximum torque indicating the formation of a higher number of cross-links. Additionally, the micro-particles markedly reduce the cure time, revealing that these ceramic micro-particles behave as vulcanizing agents for silicone, leading to an increase in the vulcanization rate.

As explained in the introduction, the electro-mechanical behavior of dielectric elastomers is determined by both their dielectric properties and their mechanical properties. Therefore, uniaxial tensile tests were performed in order to evaluate the mechanical performance of the composites (see ESI for the stress-strain curves). The experimental results (Table 1) show that the tensile stress (σ) of the neat PDMS measured at different strains (50, 100 and 300%) is retained in composites containing 2.3 and 5.1 vol.% of CCTO, while the incorporation of 8.4 vol.% of CCTO causes a slight increase in the tensile stress value. In addition, the elongation at break (e_b) of the PDMS is not significantly affected by the addition of CCTO micro-particles.

Fig.2 SEM of cryo-fracture surface of PDMS composites with (a) 2.3 vol.%, (b) 5.1 vol.%, and (c) 8.4 vol.% of CCTO. The scale bar corresponds to 20 μm.

4.2.2. Structural and Microstructural Characterization

CCTO/PDMS vulcanized samples were investigated by Scanning Electron Microscopy (SEM) and Confocal Raman Microscopy (CRM) in order to determine the particle distribution in the polymer matrix. Figure 2 clearly shows the CCTO micro-particles individually distributed within the PDMS matrix, even at the highest filler content. This fact will be of importance during the electro-mechanical experiments in order to achieve a homogenous enhancement of the actuation response while applying the voltage.

Figure 3a shows an optical microscopy image of the 5.1 vol.% CCTO/PDMS composite. The arrow labeled as AB indicates the position where the cross section Raman area has been performed (Figure3e). Figure 3b exhibits the Raman spectrum of CCTO ceramic powder from 0 to 3500 cm^{-1} and the bands associated to the TiO$_6$ octahedron vibration motions. CCTO is predicted to have eight symmetry modes but usually only five of them are observed, classified as TiO$_6$ rotation-like modes: A_g (1) (444 cm^{-1}), F_g (2) (453 cm^{-1}) and A_g (2) (510 cm^{-1}) and Ti–O–Ti stretching modes of the octahedron: F_g (3) (576 cm^{-1}) and F_g (4) (710 cm^{-1}), assigned as asymmetric and symmetric modes, respectively.[31] In the ceramic CCTO powder only three bands are detected, corresponding to the A_g (1), A_g (2) and F_g (3) modes. Raman spectra of PDMS and CCTO/PDMS composite are presented in Figures 3c and 3d, where the numbers next to the spectra indicate the vibrational peaks designation associated to the PDMS vibration atomic motions: (1) Si-O-Si symmetric stretching (496 cm^{-1}), (2) Si-CH$_3$ symmetric rocking (715 cm^{-1}), (3) Si-C symmetric stretching (798 cm^{-1}), (4) CH$_3$ asymmetric rocking + Si-C asymmetric stretching (870 cm^{-1}), (5) CH$_3$ symmetric rocking (1272 cm^{-1}), (6) CH$_3$ symmetric bending (1420 cm^{-1}), (7) CH$_3$ asymmetric bending (2920 cm^{-1}), and (8) CH$_3$ symmetric stretching (2979 cm^{-1}). These values are in good agreement with the values reported by other authors.[32] Figure 3e shows a color-coded image evidencing the regions of the sample where the Raman spectrum corresponds to the one presented in Figure 3b (red color regions) or to the Figure 3c (blue ones). This image displays the distribution of CCTO ceramic powder in the PDMS matrix. The depth profile Raman image only reaches a few microns since CCTO absorbs the laser radiation, limiting the reflectance detection. However, Raman imaging gives a clear view of the distribution of the CCTO micro-particles among the matrix and corroborates the SEM results.
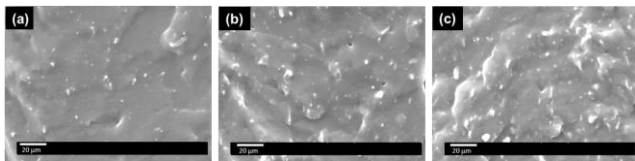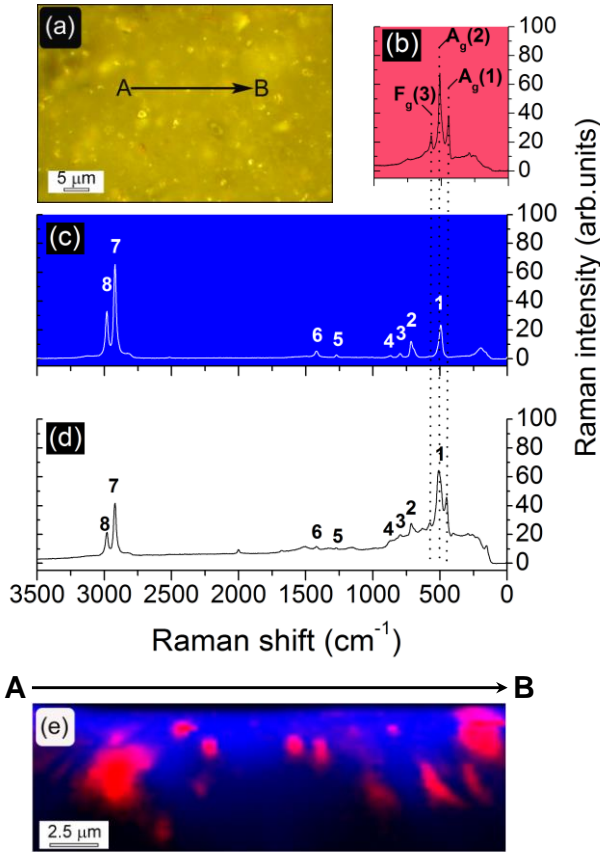
Fig. 3 Characterization of 5.1 vol.% CCTO/PDMS composite through Confocal Raman Microscopy: (a) Optical image of CCTO/PDMS composite. The arrow AB shows the position where the XZ Raman profile has been performed. (b) Raman spectrum of CCTO indicating its active modes, (c and d) Raman spectra of PDMS and CCTO/PDMS composite. The numbers next to the vibrational peaks represent the main atomic motions. (e) Raman color map showing the distribution of CCTO and PDMS in the cross section represented as an arrow in (a).

4.2.3. Dielectric Properties. Comparison with Classical Dielectric Mixing Rules

The dielectric properties of the PDMS and its composite films measured at room temperature as a function of frequency are shown in Figure 4.

Increased CCTO content leads to a substantial increase of the dielectric constant, ε', throughout the entire frequency range. More specifically, we found that a 8.4 vol.% addition of CCTO into the PDMS matrix raises the dielectric constant by 74 %, from $\varepsilon' = 3.13$ to $\varepsilon' = 5.45$ at 1 kHz. The dielectric permittivity of all the samples shows a frequency independent behavior, which indicates the absence of localized movement of charges, i.e. interfacial polarisation or Maxwell-Wagner-Sillars polarisation, within the composites and suggests that the charge remains confined in the micro-particles. This phenomenon can be ascribed to the semi-conductive character of the CCTO ceramic. Concomitantly, the dielectric loss tangent trend of the CCTO/PDMS composites remains roughly the same as for the neat PDMS (except at high frequencies). The apparent reduction of the dielectric loss tangent values is due to the large increase of the dielectric permittivity compared to the slight increment observed in the

dielectric loss constant. Hence, this result suggests that the addition of the CCTO particles does not introduce any additional loss mechanisms, confirming that there is no charge dissipation within the composites. Hence, the dielectric character of the PDMS matrix is preserved with the addition of CCTO micro-particles. The deviation observed at high frequencies could be attributed to an antenna effect of the charges in the semi-conducting particles that couple with the external electromagnetic field, increasing the spectrum noise.

Following classical dielectric mixing rules, it is possible to predict, up to a certain level, the effective dielectric permittivity of a composite. These approaches consider the composite as an isotropic medium of dielectric permittivity ε_1 and volume v_1 filled with a dielectric phase of permittivity ε_2 and volume $v_2 = 1 - v_1$.[33, 34] We have analyzed five different models, where the first two provide a rough estimate of the dielectric permittivity boundaries and the rest a finer prediction based on the Maxwell-Garnett approximation. As a starting point, it is possible to identify the lower ($\varepsilon_{c,min}$) and upper ($\varepsilon_{c,max}$) bound for the composite effective dielectric permittivity (ε_c) as:

$$\varepsilon_{c,min} = \frac{\varepsilon_1 \varepsilon_2}{\varepsilon_1 v_2 + \varepsilon_2 v_1} \qquad (2)$$

$$\varepsilon_{c,max} = \varepsilon_1 v_1 + \varepsilon_2 v_2 \qquad (3)$$

which correspond to the equivalent series and parallel model circuits, respectively.
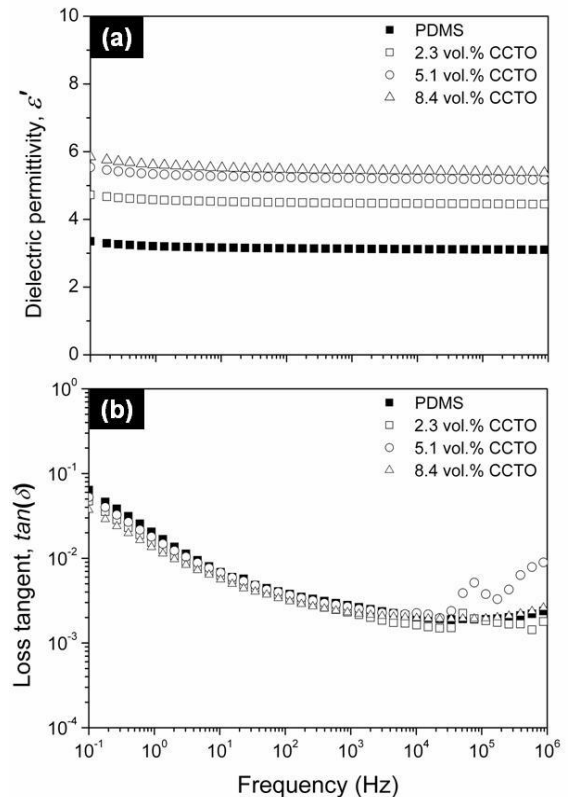
Fig. 4 Dielectric spectra for PDMS and its composites, showing: (a) the dielectric permittivity, and (b) the loss tangent.

In general, and based on the random spatial arrangements of the filler, it is expected that the effective dielectric permittivity of a composite, ε_c, will be somewhere between these two extremes. One of the oldest and most popular effective medium theory is the Maxwell-Garnett approximation, which assumes a two-phase isotropic dielectric component with spherical shaped inclusions ideally dispersed, thus defining the effective dielectric permittivity as follows:[35]

$$\varepsilon_{c\,(Maxwell-Garnett)} = \varepsilon_1 \left(1 + \frac{3v_2(\varepsilon_2-\varepsilon_1)}{2\varepsilon_1+\varepsilon_2-v_2(\varepsilon_2-\varepsilon_1)}\right) \quad (4)$$

The Bruggeman's model, which is an extension of the Maxwell-Garnett approximation, permits to assess the overall electrical response at high loading contents with the premise that the dispersed spheres do not form a percolative path through the medium and includes the polarizability of the inclusions in the calculation, resulting the following expression for the dielectric permittivity:[36]

$$\varepsilon_{c\,(Bruggeman)} = \varepsilon_2 \frac{3\varepsilon_1+2v_2(\varepsilon_2-\varepsilon_1)}{3\varepsilon_2-v_2(\varepsilon_2-\varepsilon_1)} \quad (5)$$

In our case, as shown in Figure 5, the experimental dielectric data lies somewhere between these last two mixing rules. Maxwell-Garnett and Bruggeman's models fail to predict the experimental dielectric permittivity of the developed composites mainly due to both the high dielectric contrast between the filler and the elastomeric matrix, and the non-spherical shape of CCTO micro-particles as evidenced by SEM.

The more accurate Yamada's model is based on the assumption that the polymer dielectric characteristics are very different from those of the filler and introduces a shape parameter n for non-spherical inclusions.[37] This geometry factor corresponds to $n = 3$ for spherical particles, while $n < 3$ and $n > 3$ correspond to oblate and prolate particles in the applied electric field, respectively.

$$\varepsilon_c = \varepsilon_1 \left[1 + \frac{nv_2(\varepsilon_2-\varepsilon_1)}{n\varepsilon_1+(\varepsilon_2-\varepsilon_1)(1-v_2)}\right] \quad (6)$$

The dielectric constant values (ε_1 and ε_2) used for fitting the equations were calculated from the dielectric permittivity curves at 10 Hz ($\varepsilon_1 = 3.16$ and $\varepsilon_2 = 142.92$). The experimental dielectric data at 10 Hz were found to fit reasonably well in the expression developed by Yamada for n = 12.5, which corresponds to prolate-shaped particles and is in concordance with the results reported by Prakash *et al.*[38] and Thomas *et al.*[39] for CCTO micro-particles in an epoxy and PVDF matrices, respectively. These results evidence the applicability of this model to predict effectively the dielectric characteristics of CCTO composites.
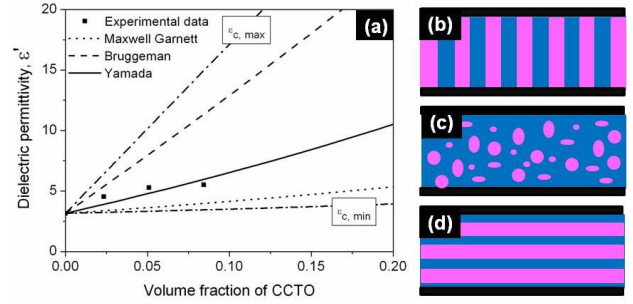
Fig. 5 (a) Experimental dielectric permittivity values (at 10 Hz) for CCTO/PDMS composites as a function of the CCTO volume fraction employed. The lines correspond to the fittings of the described models. Schematic diagram outlining the two-phase composite models: (b) parallel, (c) random and (d) series model, where the polymer is represented in blue, the filler in pink and the electrodes as black lines.

4.2.4 Electro-Mechanical Performance.

A method to systematically determine the goodness of the achieved compromise between the effect of the fillers in the dielectric permittivity and the mechanical properties is by defining a factor *f*, or electro-mechanical performance of the material.[7] As explained, the electro-mechanical response is proportional to the dielectric permittivity over the elastic deformation of the material. Thus, *f* for a given composite can be defined as the quotient of the actuation strain of the composite, S_c, and that of the matrix, S_0:

$$f = \frac{S_c}{S_o} = \frac{\varepsilon'_c Y_o}{\varepsilon'_0 Y_c} \quad (7)$$

where ε'_c and Y_c are the values of the dielectric permittivity and the tensile stress at a given strain for the composite, and ε'_0 and Y_0 for the polymer matrix. Hence, only those composites having $f > 1$ will show electro-mechanical improvements over the raw matrix. It is worth noting that *f* does not provide a quantitative evaluation of the actuator performances since the actuators are subjected to biaxial strains in the experimental set-up and the *f* ratios are obtained from uniaxial stress-strain measurements. Nevertheless, *f* values can be used as figures of merit to provide a qualitative idea about what to expect in the electro-mechanical tests. Therefore, since *f* >1 in all the cases (Table 2), the composites should *a priori* show an improved electro-mechanical response compared with the raw matrix. Moreover, the electro-mechanical performance *f* value increases with the CCTO content up to 5.1 vol.%, showing that the enhancement in the actuation properties is due to both the increment of the dielectric permittivity value and the preservation of the tensile stress at 50 and 100 % strain. Above this optimal concentration, the increase in the dielectric permittivity is not enough to overcome the increase in the stiffness of the composite, thus decreasing the electro-mechanical performance value.

The experimental actuation strain percentages for the PDMS matrix and its composites are displayed in Figure 6a as a function of the applied nominal electric field. All composite actuators show an improved performance compared with the raw elastomer, being the trend of the experimental actuation

similar to the performance *f* value previously defined. The maximum actuation sensitivity is achieved for the composite with 5.1 vol.% of CCTO. This composite shows an actuation strain of 4.01% at 20 V/µm, which is an increment in the actuation strain of about 100% and a reduction of 25% in the electric field to reach the same strain compared to the raw PDMS matrix (Figure 6b and 6c). Recently, Böse *et al.*[8] have also reported an improvement of about 100% (measured at 20 V/µm) in the actuation strain but for a 20 vol.% dried $BaTiO_3$ (particle size < 3µm)/PDMS composite. Stoyanov *et al.*[9] obtained a maximum improvement for 15 vol.% silicone oil coated TiO_2 nanoparticles/SEBS composites, with a corresponding reduction in activation fields of 27%. These results indicate that the insulated and homogeneously distributed high dielectric constant CCTO filler makes a significant contribution to the increase of the electro-mechanical performances here reported.
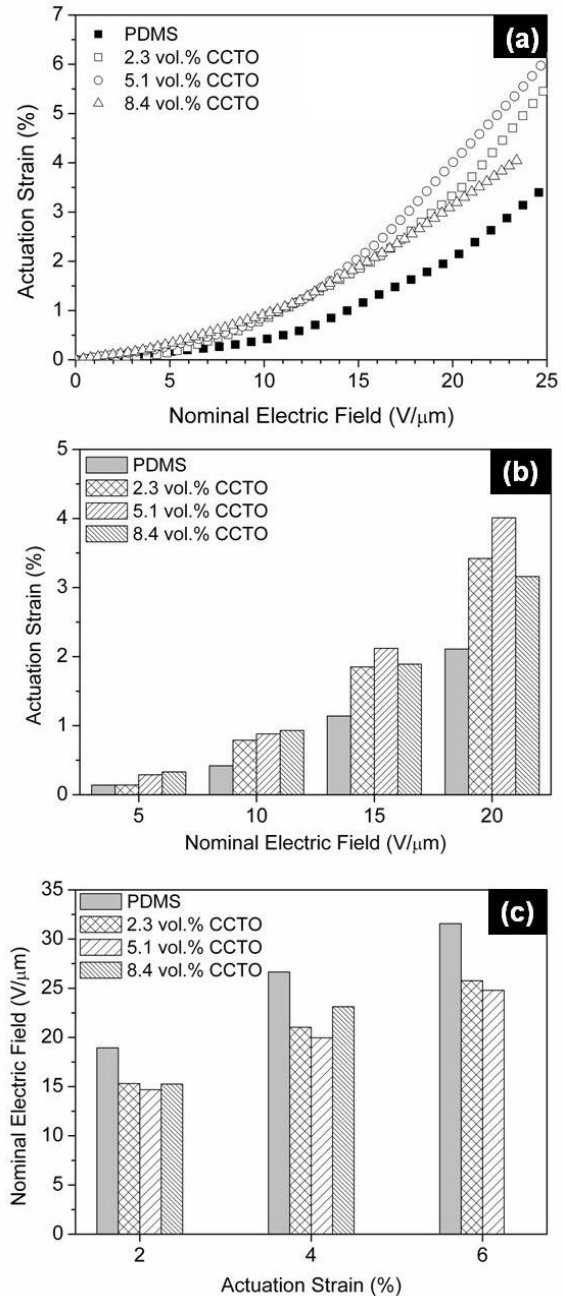
Table 2 Theoretical electro-mechanical performance

Sample	ε' at 1 kHz	*f* at 50% strain	*f* at 100% strain
PDMS	3.13	1	1
2.3 vol.% CCTO	4.48	1.41	1.38
5.1 vol.% CCTO	5.22	1.64	1.64
8.4 vol.% CCTO	5.45	1.37	1.34

The dielectric breakdown strength values (E_b), obtained from at least five independent actuator measurements, are 55.9 ± 1.8, 37.9 ± 7.8, 27.4 ± 3.9 and 23.6 ± 5.8 V/µm, for PDMS, 2.3, 5.1, and 8.4 vol.% CCTO respectively. The reduction of the breakdown strength has previously been observed in composite DEAs and has been ascribed to a possible Joule effect.[9]

Conclusions

In this work we have evaluated and shown the feasibility of using Calcium Copper Titanate $CaCu_3Ti_4O_{12}$ (CCTO) as giant dielectric constant filler in a Polydimethylsiloxane (PDMS) matrix for applications as dielectric elastomer actuators (DEAs). The composites exhibited a remarkable combination of dielectric permittivity increment and preservation of both the dielectric loss value and the tensile stress values at different strains, thus, yielding a large electro-mechanical performance for composites up to 5.1 vol.% of CCTO. These actuation performances were also found to agree reasonably well with the defined figure of merit, showing that the addition of CCTO micro-particles results in a significant improvement on the actuation sensitivity in DEAs.

Fig. 6 Experimental electro-mechanical performance of PDMS and CCTO/PDMS actuators showing: (a) actuation strain (%) as a function of the nominal electric field (each curve represents the average of at least 5 independent actuators devices), (b) actuation strains (%) at a nominal electric field of 5, 10, 15 and 20 V/µm, and (c) nominal electric field (V/µm) at 2, 4 and 6 % actuation strain.

Notes and references

[a] *Instituto de Ciencia y Tecnología de Polímeros, ICTP-CSIC, Juan de la Cierva, 3, 28006 Madrid, Spain Fax: 34 91 5644853; Tel: +34 91 562 2900; E-mail: rverdejo@ictp.csic.es; laura.jimenez@ictp.csic.es*
[b] *Instituto de Cerámica y Vidrio, ICV-CSIC, Kelsen 5, 28049, Madrid, Spain.*
[c] *Università degli Studi di Perugia, Materials Science and Technology Center, Loc. Pentima Bassa 21, 05100, Terni, Italy*
† Electronic Supplementary Information (ESI) available: X-ray diffraction patterns of both sintered and powder CCTO. Stress-strain curves of PDMS and its composites See DOI: 10.1039/b000000x/

1. R. Shankar, T. K. Ghosh and R. J. Spontak, *Soft Matter*, 2007, **3**, 1116-1129.

2. K. Gabor, L. Patrick and W. Michael, *Smart Materials and Structures*, 2007, **16**, S306.

3. C. Jordi, S. Michel, G. Kovacs and P. Ermanni, *Sens. Actuators A*, 2010, **161**, 182-190.

4. X. Niu, P. Brochu, B. Salazar and Q. Pei, Proc. SPIE, San Diego, California, USA, 2011.

5. S. Akbari and H. R. Shea, *J. Micromech. Microeng.*, 2012, **22**, 045020.

6. R. Pelrine, R. Kornbluh, Q. Pei and J. Joseph, *Science*, 2000, **287**, 836-839.

7. H. Stoyanov, M. Kollosche, D. N. McCarthy and G. Kofod, *J. Mater. Chem.*, 2010, **20**, 7558-7564.

8. H. Böse, D. Uhla, K. Flittnerb and H. Schlaakb, SPIE, San Diego, 2011.

9. H. Stoyanov, M. Kollosche, S. Risse, D. N. McCarthy and G. Kofod, *Soft Matter*, 2011, **7**, 194-202.

10. M. Molberg, D. Crespy, P. Rupper, F. Nüesch, J.-A. E. Månson, C. Löwe and D. M. Opris, *Adv. Funct. Mater.*, 2010, **20**, 3280-3291.

11. R. Pelrine, R. Kornbluh, J. Joseph, R. Heydt, Q. Pei and S. Chiba, *Mater. Sci. Eng., C*, 2000 **11**, 89.

12. Z. M. Dang, Y. Shen and C. W. Nan, *Appl. Phys. Lett.*, 2002, **81**, 4814-4816.

13. J. Lu, K. S. Moon, J. Xu and C. P. Wong, *J. Mater. Chem.*, 2006, **16**, 1543-1548.

14. H. Stoyanov, D. M. Carthy, M. Kollosche and G. Kofod, *Appl. Phys. Lett.*, 2009, **94**, 232905.

15. M.-J. Jiang, Z.-M. Dang and H.-P. Xu, *Appl. Phys. Lett.*, 2007, **90**, 042914.

16. C. Huang and Q. Zhang, *Adv. Funct. Mater.*, 2004, **14**, 501-506.

17. J. P. Szabo, J. A. Hiltz, C. G. Cameron, R. S. Underhill, J. Massey, B. White and J. Leidner, SPIE, San Diego, CA, USA, 2003.

18. G. Gallone, F. Carpi, D. De Rossi, G. Levita and A. Marchetti, *Mater. Sci. Eng., C*, 2007, **27**, 110-116.

19. M. Molberg, École Polytechnique Fédérale de Lausanne, 2010.

20. M. Arbatti, X. Shan and Z. Y. Cheng, *Adv. Mater.*, 2007, **19**, 1369-1372.

21. M. A. Subramanian, D. Li, N. Duan, B. A. Reisner and A. W. Sleight, *J. Solid State Chem.*, 2000, **151**, 323-325.

22. B. Bochu, M. N. Deschizeaux, J. C. Joubert, A. Collomb, J. Chenavas and M. Marezio, *J. Solid State Chem.*, 1979, **29**, 291-298.

23. T. B. Adams, D. C. Sinclair and A. R. West, *Adv. Mater.*, 2002, **14**, 1321-1323.

24. G. Chiodelli, V. Massarotti, D. Capsoni, M. Bini, C. B. Azzoni, M. C. Mozzati and P. Lupotto, *Solid State Commun.*, 2004, **132**, 241-246.

25. J. L. Zhang, P. Zheng, C. L. Wang, M. L. Zhao, J. C. Li and J. F. Wang, *Appl. Phys. Lett.*, 2005, **87**, 142901.

26. J. J. Romero, P. Leret, F. Rubio-Marcos, A. Quesada and J. F. Fernández, *J. Eur. Ceram. Soc.*, 2010, **30**, 737-742.

27. P. Leret, M. A. de la Rubia, F. Rubio-Marcos, J. J. Romero and J. F. Fernández, *Int. J. Appl. Ceram. Tec.*, 2011, **8**, 1201-1207.

28. G. Kofod, D. N. M. Carthy, J. Krissler, G. Lang and G. Jordan, *Appl. Phys. Lett.*, 2009, **94**, 202901-202903.

29. C. C. Homes, T. Vogt, S. M. Shapiro, S. Wakimoto and A. P. Ramirez, *Science*, 2001, **293**, 673-676.

30. J. Y. Li, X. T. Zhao, S. T. Li and M. A. Alim, *J. Appl. Phys.*, 2010, **108**, 104104.

31. D. Valim, A. G. Souza Filho, P. T. C. Freire, S. B. Fagan, A. P. Ayala and J. Mendes Filho, *Physical Review B*, 2004, **70**, 132103.

32. S. C. Bae, H. Lee, Z. Lin and S. Granick, *Langmuir*, 2005, **21**, 5685-5688.

33. A. Sihvola, *Subsurface Sensing Technologies and Applications*, 2000, **1**, 393-415.

34. Z. M. Dang, J. K. Yuan, J. W. Zha, T. Zhou, S. T. Li and G. H. Hu, *Prog. Mater. Sci.*, 2012, **57**, 660-723.

35. J. C. M. Garnett, *Philosophical Transactions of the Royal Society of London. Series A, Containing Papers of a Mathematical or Physical Character*, 1904, **203**, 385-420.

36. D. A. G. Bruggeman, *Annalen der Physik*, 1935, **416**, 665-679.

37. T. Yamada, T. Ueda and T. Kitayama, *J. Appl. Phys.*, 1982, **53**, 4328-4332.

38. B. S. Prakash and K. B. R. Varma, *Compos. Sci. Technol.*, 2007, **67**, 2363-2368.

39. P. Thomas, K. T. Varughese, K. Dwarakanath and K. B. R. Varma, *Compos. Sci. Technol.*, 2010, **70**, 539-545.

Table of content
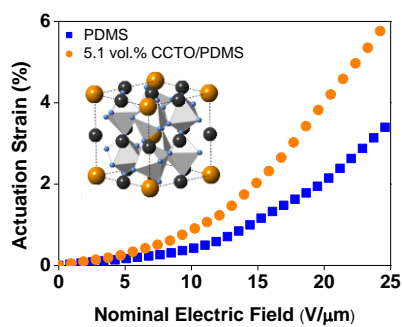
A novel Calcium Copper Titanate $CaCu_3Ti_4O_{12}$ (CCTO)/Polydimethylsiloxane (PDMS) composite with enhanced dielectric permittivity, low dielectric losses and preservation of mechanical properties was developed, making it suitable for applications in dielectric elastomer actuators.